

Decomposition with Thermo-economic Isolation Applied to the Optimal Synthesis/Design of an Advanced Tactical Aircraft System

Diego F. Rancruel and Michael R. von Spakovsky
Energy Management Institute
Department of Mechanical Engineering
Virginia Polytechnic Institute and State University Blacksburg, VA 24061
Fax: (540) 231-9100
E-mail: vonspako@vt.edu

Abstract

A decomposition methodology based on the concept of “thermo-economic isolation” and applied to the synthesis/design and operational optimization of an advanced tactical fighter aircraft is the focus of this paper. The most promising set of aircraft sub-system configurations, based on both an energy integration analysis and aerodynamic performance, were first developed and detailed thermodynamic, geometric, physical, and aerodynamic models at both design and off-design were formulated and implemented. Conceptual, time, and physical decomposition were then applied to the synthesis/design and operational optimization of the aircraft system. The physical decomposition strategy used, called Iterative Local-Global Optimization (ILGO), was developed by Muñoz and von Spakovsky (2001a,b) and has been applied to a number of complex stationary and transportation applications. This decomposition strategy is the first to successfully closely approach the theoretical condition of “thermo-economic isolation” when applied to highly complex, highly dynamic non-linear systems.

Key words: Decomposition, thermo-economic isolation, large-scale optimization, synthesis/design, aircraft systems

1. Introduction

The need for more complex, efficient, and cost effective systems makes it imperative not only to analyze a greater number of possible configurations and technologies but also to synthesize/design systems in a way which optimizes these systems taking into account load and environmental variations over time. This contrasts with the common practice of synthesizing/designing a system for a single synthesis/design point (typically chosen to be close to the most demanding operating point) followed by a verification of proper operation at off-design. Typically such single-point syntheses/designs are achieved using trade-off analysis, which utilizes a fairly non-integrated, non-interdisciplinary set of basic calculations (although at times powerful simulation tools), rules-of-thumb, and individual experience to achieve the “best” synthesis/design. In cases where optimization is considered, partially due to the fact that new and more potent computers have become available and optimization tools

more popular, it is seen as a straightforward mathematical problem, which for large-scale, highly non-linear optimization problems can be very limiting to say the least. Even significant increases in computational power are not sufficient to offset the ever increasing complexity of the ensuing synthesis/design optimization problem. In formulating this problem (i.e. identifying all the interacting sub-systems, choosing the possible configurations and decision variables, and defining the physical constraints), it may turn out that solving it as a single problem is simply impractical¹.

Such complex problems can, however, be solved as a set of smaller problems which approximate the larger one. This was done here through the use of decomposition techniques or strategies (e.g., *conceptual, time, and physical decomposition*) applied to the synthesis/design

¹ It may also be impractical due to the fact that multiple platforms and software tools as well as geographically dispersed and discipline diverse teams of engineers are involved.

optimization of an Advanced Tactical Aircraft (ATA) system. The ATA was physically decomposed into five different sub-systems with degrees of freedom. The physical decomposition approach which was used is an original decomposition strategy called Iterative Local-Global Optimization (ILGO) developed by Muñoz and von Spakovsky (2001a,b). This decomposition strategy is the first to successfully approach the theoretical condition of “thermoeconomic isolation” (Frangopoulos and Evans, 1984; von Spakovsky and Evans, 1993) when applied to highly complex, highly dynamic non-linear systems.

Finally, it should be noted that the focus of our paper is not the ATA application itself (which simply meets the need for very detailed and complex models which do a fair job of reflecting reality) but instead the original physical decomposition strategy and its ability to successfully be applied to highly complex and dynamic systems.

2. Advanced Tactical Aircraft (ATA) System Description

The advanced tactical aircraft system is decomposed into seven sub-systems of which only two (the equipment group² and the payload sub-systems) do not have any degrees of freedom although they do participate in the optimization problem through various electrical and heat loads. The ATA subsystems (see Figure 1) optimized are:

- Propulsion sub-system (PS)
- Environmental control sub-system (ECS)
- Airframe sub-system (AFS)
- Thermal Management sub-system (TMS)
 - Fuel loop sub-system (FLS)
 - Vapor compression and PAO³ loops sub-system (VC/PAOS)

The synthesis/design task at hand is to perform the integrated optimization of these five sub-systems. More specifically, what is needed is the preliminary design optimization of a low-bypass turbofan engine with afterburning (PS) and the preliminary synthesis/design optimization of an air-cycle ECS, TMS, and AFS.

The PS provides the necessary thrust for the ATA, while the AFS provides the necessary lift for the vehicle to carry out the desired mission.

² The equipment group includes flight controls, instruments, hydraulics, electrical sub-systems, avionics, furnishings, and miscellaneous empty weight.

³ Polyalphaolefin (PAO)

The mission⁴ is the set of conditions under which the aircraft must be synthesized/ designed. Here, the mission defined by the Request for Proposal (RFP) for an Air-to-Air Fighter (AAF) given by Mattingly et al. (1987) is used. The mission has 14 different segments (phases or legs). To provide the required rates of climb and acceleration and overcome the aircraft’s drag, the PS must provide the power required to operate all the remaining sub-systems. The ECS and TMS provide the cooling necessary for dissipating the heat generated in the aircraft. In modern aircraft, these cooling sub-systems face a number of challenges that are produced by high-speed flight conditions and increased internal heat loads such as those due to the avionics and those coming from the PS. A set of cooling requirements has been added to the mission according to the synthesis/design specifications given by Muñoz and von Spakovsky (1999).

3. Air Frame Sub-system (AFS) Description and Modeling

The physics of the AFS can be solved in terms of the drag polar relation and the ratio of thrust at sea level to the gross take-off weight. This physics is expressed by the flight performance master equation, which opens up the possibility for using decomposition for solving the AFS optimization sub-problem (non-energy sub-system) with those for the PS, TMS, and ECS (energy sub-systems). Moreover, the drag and the drag due to lift depend not only on flight conditions and requirements (e.g., Mach number) but also on AFS geometry and weight. The AFS⁵ in this work is defined as the empty aircraft, which includes all subsystems such as the fuselage, wings, tail, gear, etc. but excludes the fuel weight, the payload, and the equipment group. Since the PS, TMS and ECS have been defined as independent sub-systems, they are also excluded from the AFS.

The AFS has two characteristics, which are especially interesting from an optimization point of view, i.e. weight and geometry. These characteristics depend on each other (e.g., a variation of weight produces changes in the optimum geometry and changes in the geometry affect the final gross take-off weight). AFS weight and geometry are not only the basis for solving the AFS optimization sub-problem but are also the link between the AFS and the other

⁴ The mission is equivalent to the load profile and set of environmental conditions in a stationary application.

⁵ The AFS consists of the wings, tails, fuselage, landing gear, engine mounts, firewalls, engine section (but not the inner workings of the engine, i.e. the PS), and air induction sub-systems.

sub-system sub-problems. For instance, there is an effect of weight and geometry (i.e. aerodynamics, drag, and lift) on thrust for each mission segment, which in turn determines the performance requirements and constraints for the PS.

4. Environmental Control Sub-system (ECS) Description and Modeling

The air cycle of the ECS dissipates heat by transforming it into work. The most used ECS configuration is the bootstrap system due to its higher efficiency when compared to a simple air cycle. In the bootstrap system, performance is improved by using the air turbine work output for increased compression of the air upstream of the turbine. Thus, a higher compression ratio is achieved with a correspondingly higher temperature drop across the turbine. The conventional bootstrap system is shown in Figure 1. It provides conditioned air to the cockpit and avionics. The ECS performance is closely coupled with the PS and aircraft flight conditions. Changes in engine power settings cause changes in bleed air pressures and temperatures, which in turn affect the performance of the ECS. Further details about the ECS are presented in Rancruel and von Spakovsky (2003). The mass of the ECS, the amount of fuel required to carry this mass, and the fuel itself are a function of a number of factors including the flight conditions. The weight model, physical model, and thermodynamic model for each ECS component are given in Rancruel (2003). In addition, the ECS, as is the case with the TMS, introduces the following additional fuel requirements:

- To provide the additional thrust needed for carrying the mass of the ECS and the drag generated;
- To overcome any additional drag
- To carry the quantity of fuel required for the previous items.

5. Thermal Management Sub-System (TMS) Description and Modeling

The TMS considered here uses a basic vapor compression cooling cycle (sub-system), which interacts with the bootstrap ECS. This combination represents a highly complex cooling system similar to the ones used by advanced fighter aircraft and uninhabited combat air vehicles (UCAVs). The TMS has a number of other sub-systems including two Polyalphaolefin (PAO) loops and a fuel loop. The TMS provides conditioned air for the high-heat generation avionics. The TMS removes heat from the high-

heat generation avionics via the cold PAO⁶ loop. In order to approach the highly transient behavior exhibited by the TMS, it is decomposed into two sub-systems, the vapor compression / PAO loops sub-system (VC/PAOS) and the fuel loop sub-system (FLS). Figure 1 shows the VC/PAOS and the connecting streams to the other sub-systems. The energy (exergy) of Q_{fuel} , which connects this sub-system with the FLS, provides the necessary thermodynamic link between the two sub-systems. Q_{Bleed} provides the thermodynamic links between the VC/PAOS and the ECS, while the power used by the vapor compressor provides the energy (exergy) links between the VC/PAOS and the PS. The vapor compression (VC) cycle transfers heat from the cold PAO loop to one at a higher temperature (the hot PAO loop⁷). The PAO loop receives heat from the VC cycle through the condenser. Following the condenser, the PAO is pumped toward a bleed air-PAO heat exchanger where it receives heat from the bleed air. The PAO, at high temperature, is then cooled using ram air from the same scoop inlet as that used for the ECS. Before the PAO returns to the condenser, it is cooled using the aircraft fuel as a heat sink.

The FLS is shown in detail in Figure 1. The purpose of the FLS is to take advantage of the fuel heat capacity to use it as a heat sink. The operation of the FLS is dependent on the temperature of the thermal storage tank (i.e. fuel tank) and the heat loads from the PS, the hydraulics, and VC/PAOS. A detail description of the FLS is given in Rancruel and von Spakovsky (2003). The feedbacks from the VC/PAOS, the PS, and the hydraulic sub-systems are the loads imposed on the FLS, which change with the different mission segments.

6. Propulsion Sub-system Description and Modeling

The PS (see Figure 1) has eighteen components. The sub-system is a low-bypass turbofan engine with afterburning. The on- and off-design behavior of the engine is simulated using a modern performance code developed by an engine manufacturer for modeling any type of aircraft engine system. The model of the engine uses typical component maps and functional relationships and numerical constants that modify the maps to make the simulation as realistic as possible. The computer program has its own set of solvers to carry out the mass, momentum, energy, and shaft speed balances.

⁶ The cold Polyalphaolefin (PAO) loop is used as a heat sink for the vapor compression cooling cycle.

⁷ The hot Polyalphaolefin (PAO) loop is that used as the intermediate heat carrier between the vapor compression cycle and the fuel loop.

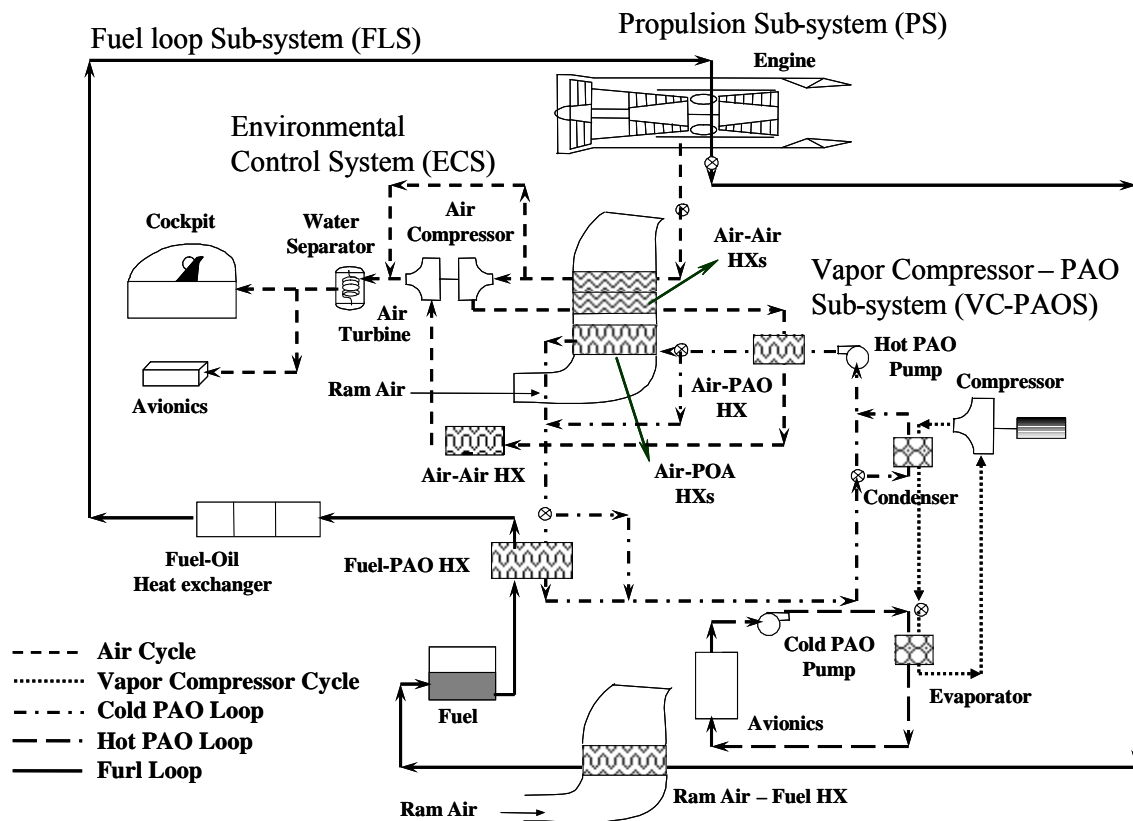


Figure 1. Energy and mass flow diagram of the ATA, excluding the AFS and the equipment group and payload sub-systems.

Results from the simulation are the thermodynamic properties at each of the engine stations (pressure, temperature, Mach number, etc.), the inlet air flow rate, nozzle areas, and the fuel consumed in the combustor and afterburner adjusted to provide the thrust required by the mission during the different segments of the mission. The weight and dimensions of the PS are calculated using the computer code Weight Analysis of Turbine Engines - WATE (WATE User Guide, 2000). WATE was originally developed by the Boeing Military Aircraft Company in 1979 and improved by NASA and the McDonnell Douglas Corporation.

Finally, a detailed presentation of the thermodynamic, aerodynamic, and geometric models developed for the PS as well as for the other sub-system configurations is beyond the scope of this paper. For details of all of these models, the reader is referred to Rancruel (2003). A diagram describing the energy and mass flows of the thermodynamic sub-system models for the complete ATA system (only the AFS and the equipment group and payload sub-systems are excluded) is shown in Figure 1.

7. Decomposition Techniques for the Synthesis/ Design Optimization of Energy Systems

7.1 System Synthesis/Design Multi-level Optimization Techniques

Conceptually, decomposition can be viewed as an interface between a designer's models, simulators, and/or analyzers and the optimization algorithms (i.e. gradient- and non-gradient based) to which they would be coupled (see Figure 2). This defines a multi-level approach, which contrasts with the traditional single-level approach in which the interface is absent. Four principal types of decomposition define such a multi-level approach: disciplinary, conceptual, time, and physical (e.g., see El-Sayed, 1989; Zimering, Burnes, Rowe, 1999; Frangopoulos, 1990; Olsommer, von Spakovsky, Favrat, 1999; Muñoz and von Spakovsky, 2001a,b, 2003; Georgopoulos, von Spakovsky, and Muñoz, 2002).

The first of these, disciplinary decomposition, decouples, for example, a problem's thermo-dynamics and economics and optimizes each discipline independently. In this work, only physical, time and conceptual decomposition are used to solve the aircraft system synthesis/design optimization problem. A brief description of each of these is given in the following sections.

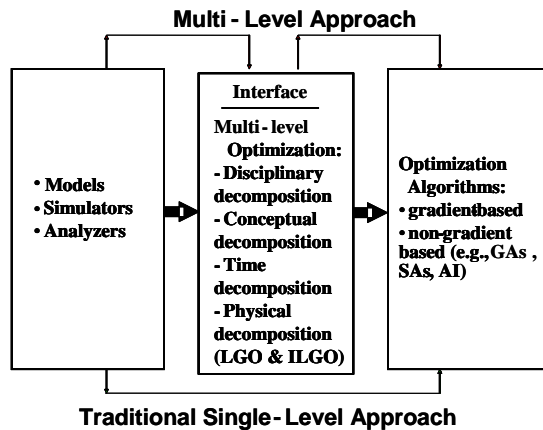


Figure 2. A conceptual view of decomposition.

7.2 Conceptual and Time Decomposition

It is essential that the synthesis/design optimization of a system be done in such a way that the system is always able to meet a certain set of loads or mission requirements over a long period of time characterized by varying environmental conditions. However, this complicates a possibly already complex optimization problem. The technique of time decomposition facilitates the solution of such a problem by dividing the time period of the entire load or mission profile into small time segments, each one representing a particular set of loads or mission requirements and its corresponding environmental conditions. Each segment then represents a single sub-problem at the operational level. Time decomposition transforms a dynamic problem into a quasi-stationary one consisting of a series of stationary time segments.

Another technique for facilitating the solution of such a problem is conceptual decomposition, which transforms the overall time-dependent problem, consisting of $d + o + \tau$ independent variables (d synthesis/design variables, o operational variables, and τ time segments) into two separate sub-problems with $d + o$ and $o(\tau - 1)$ variables, respectively. In addition, after decomposing in this fashion as well as in time, it is still possible that the complex problem of energy system synthesis/design optimization remains difficult or impossible to solve without further decomposition. In this case, an additional decomposition technique, namely physical decomposition, may be required.

7.3 Physical Decomposition

For optimization purposes, most energy systems (and some non-energy systems, e.g., the AFS) can be divided into components or sub-systems with a clearly defined set of coupling

functions⁸. The result of such a physical decomposition is a set of unit sub-problems with a much smaller size than the overall problem, making it possible to take into account a larger number of decision variables (degrees of freedom). Two approaches can be considered for solving the overall optimization problem using physical decomposition. The first is the Local-Global Optimization (LGO) approach and the second an original approach, Iterative Local-Global Optimization (ILGO), developed by Muñoz and von Spakovsky (2000). For a deeper understanding of the concepts presented in this paper, the reader is referred to the work by Muñoz and von Spakovsky (2000, 2001a,b, 2003).

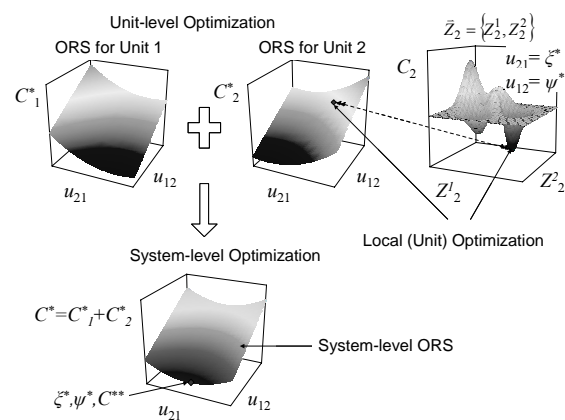


Figure 3. Unit-level and system-level optimizations and optimum response surfaces (ORSs).

In the LGO technique, a technique, which characterizes most of the decomposition approaches in the literature, two levels of optimization instead of one are used. At the local or unit level (see Figure 3), the unit sub-problems must be solved several times for different values ξ and ψ of the coupling functions u_{12} and u_{21} . A two-unit decomposition has been assumed for illustration purposes. It is furthermore assumed in using LGO that it is possible to find different sets of values for the independent variable vectors \vec{Z}_1 and \vec{Z}_2 which correspond to particular values ξ and ψ of u_{12} and u_{21} . The different solutions to the unit sub-problems for the various combinations of the coupling function values lead to a set of optimum values for the local objectives in the form of $C_1^* = C_1(\vec{Z}_1^*, \xi, \psi)$ and $C_2^* = C_2(\vec{Z}_2^*, \xi, \psi)$ where

⁸ In an energy system, the coupling functions can be considered as products, resources, and/or feedbacks going to or coming from its sub-systems. Under the right conditions, the sub-systems can then be optimized independently while maintaining these couplings between them.

\bar{Z}_1^* and \bar{Z}_2^* are the unit optimum independent variable vectors. The optimum results for the local (unit-level) objectives can be plotted versus the coupling functions. The surfaces created in this way are called unit-level optimum response surfaces (ORSs). At the global or system level, the system synthesis/design is optimized with respect to the coupling function values. A set of optimum values for the system-level objective function, C^* , results from combinations of the sum of the optimum solutions found by solving the unit-level sub-problems. The graphical representation of this set of system-level optimum values versus the coupling functions is called the system-level optimum response surface⁹ of the overall synthesis/design problem. The minimum among these optimum values, i.e. $C^{**} = C^*(\xi^*, \psi^*)$, is the one that will determine the final synthesis/design of the system.

The drawback to applying LGO is the computational burden that this decomposition approach has for large, complex systems. ILGO, on the other hand, gets around the computational burden of having to generate the system-level ORS implicitly or explicitly by using shadow price information. The *shadow prices* (von Spakovsky and Evans, 1993) indicate the relative importance of changes in the coupling functions in terms of the overall system-level objective. Geometrically, the shadow prices represent the slopes of the unit-level ORSs at the local or unit-level optimum points relative to the coupling functions. Thus, using this slope information, the system-level ORS can be searched for the global (system-level) optimum¹⁰ without having to implicitly or explicitly create the ORS. ILGO, furthermore, makes possible the decentralized, integrated synthesis/design optimization of systems by allowing multiple platforms and software tools as well as geographically dispersed and discipline diverse teams of engineers to effectively interact both at the unit (local) and the system (global) levels.

⁹ For a system with more than two coupling functions, the ORS is in fact a hyper-surface.

¹⁰ It should be noted that reference to a “global optimum” here is not meant to be taken in a strictly mathematical sense, i.e. the concern here is not in proving that decomposition necessarily leads to a Kuhn-Tucker point, but instead that in using decomposition coupled to mathematical optimization that the synthesis/design of the system as a whole can be improved even for very complex, highly dynamic problems involving a large number of degrees of freedom. If this “global” or “system-level” optimum (improvement) happens to coincide with a Kuhn-Tucker point, that is all to the better. However, the impracticality of proving this for very large and complex problems of practical interest is simply a waste of time since we are concerned here with system-level (global) and unit-level (local) improvements in synthesis/design and not mathematical proofs

One of the most appealing features of ILGO is its ability to provide the information necessary to simply improve an existing synthesis/design. In fact, in engineering practice, the word “optimization” is often used not to indicate the search for the global optimum but rather to find a solution that is better than some existing one. Thus, ILGO is a significant advance over LGO in that it

- Eliminates the nested optimizations required in standard LGO approaches. This in fact leads to what in the thermoeconomic literature is called a close approach to “thermoeconomic isolation” (Frangopoulos and Evans, 1984; von Spakovsky and Evans, 1993; Rancruel, 2003).
- Uses an intelligent search based on shadow prices to effectively search the system-level optimum response surface without having to actually generate it or the unit-level ORSs.
- Assures consistency between all local objectives and the system-level objective.
- Introduces no constraint inconsistencies from one sub-problem to another.
- Is conducive to the parallelization of the various sub-problem optimizations.

8. Optimization Strategy for the Advanced Tactical Aircraft

The system-level synthesis/design and operational optimization problem for the proposed ATA is defined as Minimize

$$W_{TO} = W_{AFS} + W_{PS} + W_{ECS} + W_{TMS} + W_{FUEL} + W_{EG} + W_{PPAY} + W_{EPAY} \quad (1)$$

w.r.t.

$$\{\bar{X}_{PS}, \bar{Y}_{PS}\}, \{\bar{X}_{ECS}, \bar{Y}_{ECS}\}, \{\bar{X}_{TMS}, \bar{Y}_{TMS}\}, \{\bar{X}_{AFS}, \bar{Y}_{AFS}\}$$

$$\text{subject to } \bar{H}_{PS} = 0, \quad \bar{G}_{PS} \leq 0 \quad (2)$$

$$\bar{H}_{ECS} = 0, \quad \bar{G}_{ECS} \leq 0 \quad (3)$$

$$\bar{H}_{TMS} = 0, \quad \bar{G}_{TMS} \leq 0 \quad (4)$$

$$\text{and } \bar{H}_{AFS} = 0, \quad \bar{G}_{AFS} \leq 0 \quad (5)$$

where the vectors of equality constraints \bar{H} represent the thermodynamic and physical models for each of the sub-systems. The vectors of inequality constraints \bar{G} represent the physical limits placed on independent and dependent variables or other physical quantities.

W_{EG} , the weight of the equipment group, and the payload weights, W_{PPAY} and W_{EPAY} , are fixed and, thus, do not participate in the

optimization. The remaining terms in the objective consist of the weight of each of the sub-systems being optimized plus the weight of the fuel. \bar{X} is the set of synthesis-design decision variables for each sub-system, which refer to the location and geometry of a component. \bar{Y} is the set of operational decision variables, which are related to the components thermodynamics. It is important to observe that although minimization of gross take-off weight (W_{TO}) is not a thermoeconomic objective unless the two are linearly related, it, nonetheless, shares many of its characteristics. For example, the synthesis/design and operation of any given sub-system forces the sub-systems with which it interacts to change their size. In the present problem, that change is reflected in different weights.

8.1 Appropriate selection of the Coupling Functions

The material and energy streams linking the five sub-systems (units) of the ATA are the coupling functions used in ILGO. In applying ILGO to the system-level optimization problem for gross takeoff weight, one unit-level optimization problem is defined (i.e. ILGO-A is applied to the PS) and four unit-based, system-level optimization problems (i.e. ILGO-B is applied to the ECS, VC/PAOS, FLS, and AFS)¹¹. The coupling functions which along with their associated shadow prices are used in ILGO to eliminate the system-level optimization problem of LGO by incorporating system-level information directly at the unit level include among others the power for the VC/PAOS; the bleed air for the ECS; the drag penalties for the ECS, VC/PAOS, and FLS; the masses of the VC/PAOS, the FLS, and ECS; and the ECS bleed port selection.

8.2 ECS Unit-based, System-level Optimization Problem Definition

The ECS unit-based, system-level optimization problem is formulated as Minimize

$$W'_{ECS} = W_{TO} = W_{ECS} + W^*_{AFS} + W^*_{TMS} + W^*_{EPAY} + W^*_{PPAY} + W^*_{PS} + W^*_{FUEL}$$

¹¹ Note that ILGO-A and ILGO-B are simply two different versions of ILGO. Applying the former assumes that the local or unit-level objective for a given sub-system requires only unit-level information for convergence of ILGO. Applying the latter assumes that system-level information (through the use of shadow prices and corresponding changes in the coupling functions) must be imbedded in the unit-level objective for convergence. When this is done, the objective becomes a unit-based, system-level objective. For more detail refer to Rancruel (2003) and Muñoz and von Spakovsky (2001a,b).

$$+ \sum_{i=1}^n \begin{pmatrix} \lambda \dot{m}_{Bleed_{ECS_i}} \dot{m}_{Bleed_{ECS_i}} \\ + \lambda \dot{Q}_{ECS-VC/PAOS_i} \dot{Q}_{ECS-VC/PAOS_i} \\ + \lambda D_{ECS_i} D_{ECS_i} + \lambda W_{ECS-PS_i} W_{ECS} \\ + \lambda W_{ECS-AFS_i} W_{ECS} \end{pmatrix} \quad (6)$$

w.r.t. $\{\bar{X}_{ECS}, \bar{Y}_{ECS}\}$

$$\text{subject to } \bar{H}_{ECS} = \bar{0}, \bar{G}_{ECS} \leq \bar{0} \quad (7)$$

The ECS unit-based, system-level problem represents the minimization of the ECS's unit-level objective function, while taking into account system-level information. Apart from the ECS local objective function, the expression for the ECS unit-based, system-level objective function includes local contributions, fixed values of the other local sub-system objectives and five additional terms (in the summation) that indicate the impact that variations in the ECS decision variables have on the local objectives of the other sub-systems. The terms in the summation include the shadow prices and corresponding coupling function changes associated with the ECS. These shadow prices are defined as

$$\lambda \dot{m}_{Bleed_{ECS_i}} = \frac{\partial W^*_{TO_{PS}}}{\partial \dot{m}_{Bleed_{ECS_i}}} \quad (8)$$

$$\lambda D_{ECS_i} = \frac{\partial W^*_{TO_{PS}}}{\partial D_{ECS_i}} \quad (9)$$

$$\lambda W_{ECS-PS_i} = \frac{\partial W^*_{TO_{PS}}}{\partial W_{ECS}} \quad (10)$$

$$\lambda \dot{Q}_{ECS-VC/PAOS_i} = \frac{\partial W^*_{TO_{VC/PAOS}}}{\partial \dot{Q}_{ECS-VC/PAOS_i}} \quad (11)$$

$$\lambda W_{ECS-AFS_i} = \frac{\partial W^*_{TO_{AFS}}}{\partial W_{ECS}} \quad (12)$$

The shadow prices represent marginal changes in the optimum values of the sub-system gross take-off weights due solely to marginal changes in the value of the ECS coupling functions.

8.3 VC/PAOS Unit-based, System-level Optimization Problem Definition

The unit-based, system-level optimization problem for the VC/PAOS sub-system is

Minimize

$$W'_{VC/PAOS} = W_{TO} = W_{VC/PAOS} + W^*_{AFS} + W^*_{ECS} + W^*_{FLS} + W^*_{EPAY} + W^*_{PPAY} + W^*_{PS} + W^*_{FUEL}$$

$$+ \sum_{i=1}^n \begin{pmatrix} \lambda \dot{E}_{VC/PAOS-PS_i} \dot{E}_{VC/PAOS-PS_i} \\ + \lambda D_{VC/PAOS_i} D_{VC/PAOS_i} \\ + \lambda W_{VC/PAOS-PS_i} W_{VC/PAOS} \\ + \lambda \dot{Q}_{ECS-VC/PAOS_i} \dot{Q}_{ECS-VC/PAOS_i} \\ + \lambda \dot{Q}_{FLS-VC/PAOS_i} \dot{Q}_{FLS-VC/PAOS_i} \\ + \lambda W_{VC/PAOS-AFS_i} W_{VC/PAOS} \end{pmatrix} \quad (13)$$

w.r.t. $\{\bar{X}_{VC/PAOS}, \bar{Y}_{VC/PAOS}\}$

$$\text{subject to } \bar{H}_{VC/PAOS} = \bar{0}, \quad \bar{G}_{VC/PAOS} \leq \bar{0} \quad (14)$$

8.4 FLS Unit-based, System-level Optimization Problem Definition

The unit-based, system-level optimization problem for the FLS sub-system is defined as Minimize

$$\begin{aligned} W'_{FLS} = W_{TO} = & W_{FLS} + W^*_{AFS} + W^*_{ECS} + W^*_{VC/PAOS} \\ & + W^*_{EPAY} + W^*_{PPAY} + W^*_{PS} + W^*_{FUEL} \\ & + \sum_{i=1}^n \left(\lambda \dot{E}_{FLS-PS_i} \dot{E}_{FLS-PS_i} + \lambda D_{FLS_i} D_{FLS_i} \right. \\ & \left. + \lambda W_{FLS-PS_i} W_{FLS} + \lambda W_{FLS-AFS_i} W_{FLS} \right) \end{aligned} \quad (15)$$

w.r.t. $\{\bar{X}_{FLS}, \bar{Y}_{FLS}\}$

$$\text{subject to } \bar{H}_{FLS} = \bar{0}, \quad \bar{G}_{FLS} \leq \bar{0} \quad (16)$$

8.5 AFS Unit-based, System-level Optimization Problem Definition

The unit-based, system-level optimization problem for the AFS sub-system is defined as Minimize

$$\begin{aligned} W'_{AFS} = W_{TO} = & W_{AFS} + W^*_{VC/PAOS} + W^*_{ECS} \\ & + W^*_{FLS} + W^*_{EPAY} + W^*_{PPAY} + W^*_{PS} + W_{FUEL} \\ & + \sum_{i=1}^n \left(\lambda D_{AFS_i} \Delta D_{AFS_i} + \lambda W_{AFS_i} \Delta W_{AFS_i} \right) \end{aligned} \quad (17)$$

w.r.t. $\{\bar{X}_{AFS}, \bar{Y}_{AFS}\}$

$$\text{subject to } \bar{H}_{AFS} = \bar{0}, \quad \bar{G}_{AFS} \leq \bar{0} \quad (18)$$

This unit-based, system-level objective function is comprised of local contributions, fixed values of the other subsystem objectives and four additional terms (in the summation term) that indicate the impact that variations in the AFS decision variables have on the local objective of the other sub-systems.

8.6 PS Unit-level Optimization Problem Definition

The unit-level optimization problem for the PS sub-system is

Minimize

$$\begin{aligned} W'_{PS} = W_{TO} = & W_{PS}(W_{TO}) + W^*_{AFS} + W^*_{EGS} + W^*_{ECS} \\ & + W^*_{TMS} + W_{FUEL} + W^*_{PPAY} + W^*_{EPAY} \end{aligned} \quad (19)$$

w.r.t. $\{\bar{X}_{PS}, \bar{Y}_{PS}\}$

$$\text{subject to } \bar{H}_{PS} = \bar{0}, \quad \bar{G}_{PS} \leq \bar{0} \quad (20)$$

This unit-level objective function is comprised of the local contribution ($W_{PS}(W_{TO})$), the AFS contribution ($W_{AFS}(W_{TO}, W_{PS})$), and fixed values of the other sub-system objectives.

8.7 Solution Approach

Application of conceptual, time, and physical decomposition (ILGO in particular) to the complex problem of ATA synthesis/design optimization requires an optimization procedure. Such a procedure leads to the identification of the final synthesis/design that minimizes the total gross take-off weight of the ATA over the entire mission profile. A detailed description of this procedure is presented in Rancruel and von Spakovsky (2003) and Rancruel (2003).

All of the optimization problems were solved using the commercial optimization package iSIGHT (1999). Each ILGO iteration typically consists of two steps. The first uses a Genetic Algorithm (GA) in order to effectively deal with the mixed integer variables and possible local minima problems in each of the sub-system optimizations. Each GA optimization has a minimum population size equal to three times the number of variables with a minimum of 100. The minimum number of iterations for the PS and 1000 times the population size for the VC/PAOS, FLS, AFS, and the ECS optimization problems. In the first step, the convergence criterion for the calculation of the gross take-off weight is set at 0.2 %. The second step uses the top two or three solutions obtained with the GA to narrow down the best solutions using a gradient-based algorithm (Method of Feasible Directions). For the second step, the convergence criterion on the gross take-off weight calculation is set at 0.1 %.

9. Results and Discussion

The ATA was optimized using ILGO and a total of 493 synthesis, design, and operational decision variables. These variables consisted of a mix of continuous and discrete variables. For each iteration of ILGO, TABLE I shows the weights for the PS, AFS, ECS, VC/PAOS, and FLS unit-level and unit-based, system-level optimization problems. What is believed to be the global (system-level) optimum¹² value for the

¹² See footnote 9.

total gross take-off weight of the aircraft system, W_{TO} , is obtained in seven iterations of ILGO. A significant improvement (13.07%) in the value of the system-level objective function is observed upon completion of the second ILGO iteration. The final gross take-off weight (the system-level objective function at the seventh iteration) is lower by 2920 kg than that of the first iteration, i.e. a 28.68% decrease.

TABLE I. OPTIMUM VALUES OF THE ATA AND SUB-SYSTEM WEIGHTS FOR EACH ITERATION OF THE ILGO APPROACH.

ILGO Iter. No.	W_{TO} (kg)	W_{PS} (kg)	W_{ECS} (kg)	W_{AF} (kg)	W_{FLS} (kg)	$W_{VC/PAOS}$ (kg)
1	1310	152	450	420	560	410
2	1140	126	360	360	460	320
3	1080	114	305	340	390	270
4	1045	111	280	320	340	250
5	1035	106	270	314	330	242
6	1020	104	265	310	322	237
7	1018	103	260	310	319	232

The evolution of some representative coupling functions at the synthesis/design point is given for each iteration of the optimization procedure in TABLE II. It was found that the effect of ECS weight is significantly higher than that of heat rejection, bleed air flow rate, and momentum drag. Thus, the optimum ECS solution is expected to have the smallest possible value of weight. A similar analysis yields the same conclusion for the VC/PAOS and the FLS. Regarding the VC/PAOS, all of the shadow prices have positive values, which indicates that a solution with lower power extraction, heat rejection, and drag will be preferred for a given value of VC/PAOS weight. With respect to the AFS, the relationship between total drag and weight becomes evident by analyzing the flight performance master equation. On the PS side, an optimum solution with the highest possible turbine inlet temperatures is found.

Relatively fast convergence of ILGO depends on the constant behavior of the shadow prices over relatively large ranges of the coupling function values. This is, in fact, the case as illustrated by the planar behavior of the system-level ORS (a hyper-surface) depicted in six of a total of fourteen dimensions in Figures 4 and 5. In Muñoz and von Spakovsky (2000, 2001a), it was theorized that relatively constant shadow prices would lead to the final solution in only one iteration, i.e. would achieve “thermoeconomic isolation”. This was not the case in this application, primarily due to the initial mismatch between the coupling functions for the different sub-systems, e.g., bleed conditions used in the ECS optimization, electric

power used by the VC/PAOS optimization, and those obtained from running the PS optimization. Nonetheless, a very close approach to “thermoeconomic isolation” was achieved. In fact, all the coupling function shadow prices were found to be constant over large ranges for both synthesis/design and off-design conditions, which also indicates that an adequate selection of coupling functions was made.

TABLE II. REPRESENTATIVE COUPLING FUNCTION VALUES AT THE SYNTHESIS/DESIGN POINT FOR EACH ITERATION OF ILGO.

ILGO Iter No.	D_{ECS} (N)	W_{ECS} (kg)	bleed (kg/s)	$D_{VC/PAOS}$ (N)	$W_{VC/PAOS}$ (kg)
1	332	450	0.85	130	410
2	310	360	0.79	150	320
3	306	305	0.65	0	270
4	263	280	0.61	0	250
5	232	270	0.59	0	242
6	222	265	0.57	0	237
7	220	260	0.57	0	232

Now, as to that part of the system-level ORS shown in Figure 4, it is a three-dimensional graphical representation of the optimum values of the gross take-off weight with respect to the FLS weight and the ECS weight. Based on what was stated above, it comes as no surprise that the global (system-level) optimum corresponds to the minimum FLS and ECS weights. Nevertheless, it is worth noticing that the planar behavior of the ORS results from two coupling functions belonging to two different sub-systems, which do not share any direct product or feedback. The flat behavior of the surface is consistent with the fact that the values of the weight related shadow prices remain effectively constant during the optimization process, which agrees perfectly with Muñoz (2000).

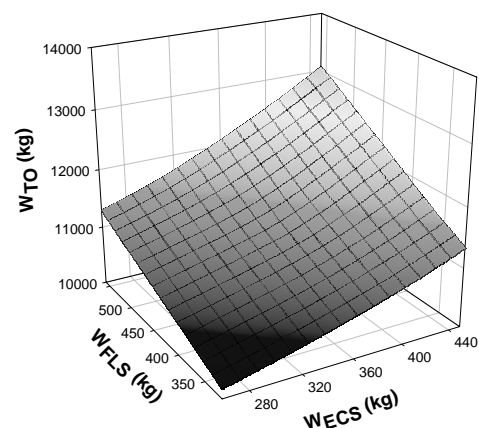


Figure 4. The ATA system-level ORS in the W_{ECS} and W_{FLS} dimensions.

Figure 5 shows the system-level objective function, W_{TO} , as a function of the ECS weight and drag. This figure has several interesting

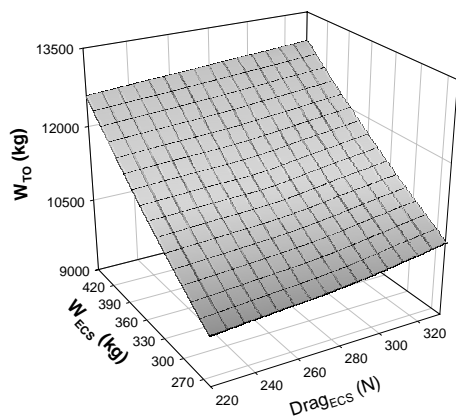


Figure 5. The aircraft system-level ORS in the W_{ECS} and D_{ECS} dimensions.

features. The first is the fact that the synthesis/design space in the ECS drag and weight dimensions is not only convex but shows flat behavior, typical of a linear system¹³. The second important feature is that this figure shows that the impact of the ECS weight on the objective function is greater than that of the ECS drag. It is important to note that the linearity mentioned above was obtained by representing the coupling functions with properties that were non-exergy or even non-energy-based. The properties used resulted not only in linear behavior but also eased calculation of the shadow prices. This essential feature of a non-energy coupling function suggested the possibility of linking the energy based sub-system syntheses/designs with that for the non-energy based sub-system (i.e. the AFS) synthesis/design. A similar analysis of the VC/PAOS and the FLS lead to a similar conclusion.

We now briefly turn to some of the results related to the local or unit-level decision variables. Two synthesis decision variables were introduced into the VC/PAOS unit-based, system-level, optimization problem. These were the location and placement of the ram-air heat exchanger. The final optimization results show that the global (system-level) optimum is reached for the VC/PAOS with no ram-air heat exchanger. One of the purposes of introducing synthesis decision variables into the VC/PAOS unit-based, system-level optimization problem was to prove the capability of success-fully using ILGO in noncontiguous synthesis/ design spaces. Two important characteristics of ILGO

¹³ It must be stressed that the objective function is linear with respect to the coupling functions and not with respect to the individual sub-system independent variables i.e. the unit-level decision variables.

permitting this are its capability to measure the effects that changes in any sub-system have on the other sub-systems and on the global objective function, and the fact that ILGO works perfectly with genetic algorithms, which can be very effective in the search of such a space.

9.1 Most Promising Syntheses/Designs and their Off-design Behavior

The conceptual decomposition approach used by Muñoz and von Spakovsky (2001a,b) is used in this work. It must be implemented in two stages. First, a synthesis/design point is chosen to guarantee that the most demanding conditions are met. In the case of the ATA, this is the most stringent mission segment for each sub-system. In the case of the FLS and AFS no conceptual decomposition was used.

For the cases of the ECS and VC/PAOS, an initial synthesis/design optimization for the most stringent point yields a set of feasible solutions which can then be evaluated at all of the other operating conditions (i.e. mission segments). Based on the instantaneous objective function value at the synthesis/design point, a ranking of feasible solutions can be created.

9.2 Results for the Final Optimum Synthesis/Design

The results presented below allow us to have some insight into the optimal synthesis and operation of the final optimum ATA synthesis/design over the entire mission profile. Complete details for all 493 degrees of freedom are found in Rancruel (2003). The aerodynamic variables have, in general, multiple effects on the global objective function. These effects are well known for the system at hand. However, the magnitudes of these effects are not easy to establish. Therefore, the usage of an inclusive aero-thermodynamic software like the one developed in-house is absolutely essential for being able to evaluate the effects that aerodynamic variable changes have on flight performance, take-off gross weight, fuel weight, component weight, etc. The optimal values for the AFS geometric decision variables are shown in Figure 6. A trapezoidal as opposed to delta wing was chosen by the optimization for the optimal shape of the ATA, consistent with the optimal L/D characteristics corresponding to the minimum WTO.

The challenge for the FLS optimization is that of finding out the sub-system synthesis/design and operational conditions, which yield the minimum sub-system weight, drag generation, and power consumption, while meeting the sub-system requirements as energy carrier and heat sink.

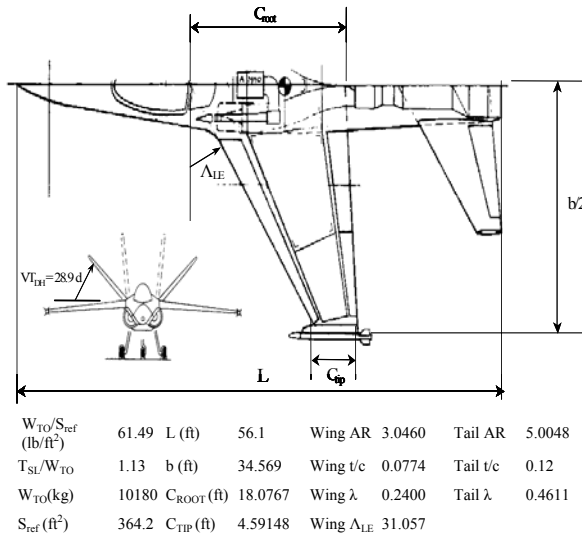


Figure 6. Optimum aircraft dimensions.

Figure 7 shows the fuel tank temperature versus time. This figure shows the advantage of using the fuel as a heat sink consistent with the FLS configuration and control strategy used in this work. Notice that at the beginning of the mission fuel consumption is higher than the require fuel flow through any of the FLS heat exchangers. Thus, all the fuel heated going through the sub-system is directed to the PS and burned and no fuel comes back to the tank, avoiding any heating (i.e. any temperature rise). After these segments, the rate of temperature rise is small, since the fuel mass at the fuel tank is still large enough. During the combat segments, the fuel consumption is also sufficiently large to deplete all the fuel going to the PS; and, thus, again the fuel tank temperature remains constant. This obviously has the additional advantage of raising the fuel temperature entering the PS. No extra fuel is passed by the ram/fuel heat exchanger during the supersonic mission segments since at these conditions the ram air cooling capabilities are particularly small. After the combat segments, which have elevated fuel consumption, the amount of fuel in the tank is greatly diminished. Thus, its heat sink capabilities are greatly reduced. Therefore, the fuel tank temperature

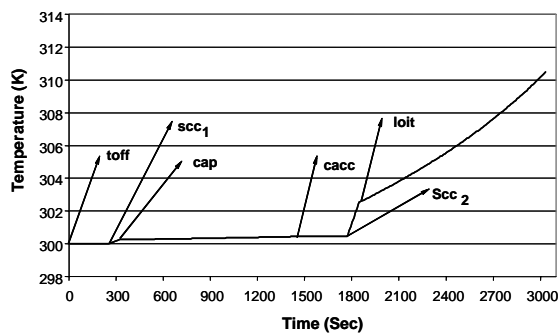


Figure 7. Fuel tank temperature versus time.

increment rate is particularly high. However, this coincides with the mission segments during which the ram-air cooling capabilities are sufficient. Therefore, with this optimization, fuel tank usage as a heat sink is maximized, since the final fuel temperature is the highest possible, without exceeding its vaporization temperature.

Finally, TABLE III shows the PS, FLS, VC/PAOS, AFS, and ECS optimum objective function values and weights. A more detailed catalogue of optimal weights for the various parts of the aircraft can be found in Rancruel and von Spakovsky (2003).

TABLE III. PS, FLS, VC/PAOS, AFS, AND ECS OPTIMUM OBJECTIVE FUNCTION VALUES AND WEIGHTS IN KG.

W_{TO} /g (kg)	10180
W_{FUEL} /g	3270
W_{EMPTY} /g	3855
$W_{PAYLOAD}$ /g	1209
$W_{Equipment}$ /g	755
W_{ECS} /g	260
ΔW_{TOECS} /g (kg)	800
$\Delta W_{FUELECS}$ /g	540
W_{FLS} /g	319.5
ΔW_{TOFLS} /g (kg)	881
$\Delta W_{FUELFLS}$ /g	561.5
W_{AFS} /g	3100
W_{ENG} /g	1032
$W_{VC/PAOS}$ /g	232
$\Delta W_{TOVC/PAOS}$ /g (kg)	622.2
$\Delta W_{FUELVVC/PAOS}$ /g	390.2

10. Conclusions

A number of conclusions on the effectiveness of the optimization and decomposition techniques presented here as well as some of the principal conclusions derived from the large-scale optimization of the ATA are as follow:

1. In previous work (e.g., Muñoz, 2000; Georgopoulos, 2002), the ability of ILGO to handle large-scale mixed integer nonlinear programming (MINLP) problems for complex transportation and stationary energy system applications was demonstrated. This has been reinforced by the application presented in this paper, which is based on Rancruel (2003). This is the most complex application to date and demonstrates not only the power of ILGO but its ability to include non-energy sub-systems (e.g., the AFS) in the optimization process as well.
2. The linear (planar) and relatively smooth behavior of both the unit-level and system-level ORS's shows that the appropriate selection of coupling functions was made.
3. The linearity of the system-level ORS is a significant contributing factor to the relatively fast convergence of ILGO.

4. ILGO is the first decomposition strategy to successfully closely approach the theoretical condition of “thermoeconomic isolation” when applied to highly complex, highly dynamic, non-linear systems. This contrasts with past attempts to approach this condition, all of which were applied to very simple systems under very special and restricted conditions such as those requiring linearity in the models and strictly local decision variables.

5. Decomposition has the advantage of breaking the overall optimization problem into a set of smaller sub-problems, which simplifies a highly complex, non-linear problem of synthesis/design optimization and allows one to take into account a larger number of decision variables (degrees of freedom) than would otherwise be possible.

6. Physical decomposition (ILGO in particular) permits the use of multiple platforms and software tools as well as the involvement of geographically dispersed and discipline diverse teams of engineers.

7. Time decomposition greatly decreases the time required for the overall optimization procedure by allowing the various off-design optimization problems to be solved simultaneously once the most promising sub-system syntheses/designs have been identified.

8. The final optimum ATA configuration is unique since geometric as opposed to thermodynamic variables were used as decision variables. The optimum AFS geometry for the given mission corresponds to a trapezoidal wing, which yields the minimum gross take-off weight and the minimum fuel consumption for the specified mission.

9. The optimum configuration for the VC/PAOS is the one without a ram-air heat exchanger. Therefore, the optimum heat sink for this sub-system is the FLS.

10. The FLS is optimized in such a way that the fuel never reaches its vaporization temperature. It does this while satisfying all the VC/PAOS cooling requirements.

11. An optimum gross take-off weight of 23,800 lb (10,799 kg) was found for the ATA without AFS degrees of freedom. This is reduced to 22,396 lb (10,162 kg), i.e. by 1404 lb (637 kg), when AFS degrees of freedom are included.

Nomenclature

ATA	Advanced Tactical Aircraft
AFS	Air Frame Sub-system
AR	Tail aspect ratio, wing aspect ratio
b	See Figure 7
bleed	ECS bleed
C	Objective function, cost

\dot{C}	Cost rate
cacc	Combat acceleration
cap	Combat air patrol
CROOT	See Figure 7
CTIP	See Figure 7
d	Number of synthesis/design variables
D	Drag
\dot{E}	Energy rate or power
EG	Equipment group
ECS	Environmental Control Sub-system
EPAY	Expendable payload
g	Acceleration of gravity
\vec{G}	Vector of inequality constraints
\vec{H}	Vector of inequality constraints
L	Fuselage length
loit	Loiter
\dot{m}	Mass flow rate
o	Number of operational variables
PPAY	Permanent payload
PS	Propulsion Sub-system
\dot{Q}	Heat transfer rate
Sref	Wing planform area
SL	Sea level
scc1	Subsonic cruise climb (1st segment)
scc2	Subsonic cruise climb (2nd segment)
t/c	Tail thickness ratio, wing thickness ratio
toff	Take-off
TSL	Sea level thrust
VC/PA	Vapor Compressor and PAO Loops
OS	Sub-system
u	Coupling function
W	Weight, fuselage width
WTO	Gross take-off weight
u	Coupling function
W	Weight, fuselage width
X	Vector of synthesis/design variables
Y	Vector of operational variables
Z	Capital function (weight, cost)

Greek

λ	Shadow price
λ	Tail taper ratio, wing taper ratio
Λ_{LE}	Wing sweep leading edge angle
τ	Number of time segments into which the set of load/environmental conditions is divided
ξ	Value of a coupling function
ψ	Value of a coupling function

Superscripts

**	Optimum
*	Restricted optimum

Subscripts

decs	ECS drag
wecs	ECS weight

References

- El-Sayed Y., 1989, "A Decomposition Strategy for Thermo-economic Optimization," *ASME Journal of Energy Resources Technology*, vol. 111, pp 1-15.
- Frangopoulos, C. A. and Evans R. B., 1984, "Thermo-economic Isolation and Optimization of Thermal System Components", *Second Law Aspects of Thermal Design*, HTD Vol. 33, ASME, N. Y., N. Y., August.
- Figliola R. S., et al., 1997. Thermal Optimization of the ECS on an Aircraft with an Emphasis on System Efficiency and Design Methodology. Soc. of Auto. Engineers, Inc. 971241 pp 137-143.
- Georgopoulos, N., von Spakovsky, M. R., Muñoz, J.R., 2002, "A Decomposition Strategy Based on Thermo-economic Isolation Applied to the Optimal Synthesis/Design and Operation of a Fuel Cell Based Total Energy System," *International Mechanical Engineering Congress and Exposition – IMECE'2002*, ASME Paper No. 33320, N.Y., N.Y., November.
- Hudson W. A. and Levin M. L., 1986. Integrated Aircraft Fuel Thermal Management. Rockwell International Corp. El Segundo, CA. Aerospace Environmental Systems, Sixteenth ICES Conference. San Diego, pp 11-25.
- gPROMS, 2000, User Guide, Version 1.8.4, Process Systems Enterprise Ltd., London, UK.
- iSIGHT, 1999, User Guide, Version 5, Engineous Software Inc., Morrisville, N.C.
- Mattingly, J.D., Heiser, W.H. and Daley, D.H., 1987, Aircraft Engine Design, AIAA Education Series, New York, New York.
- Muñoz, J. R., 2000, "Optimization Strategies for the Synthesis/Design of Highly Coupled, Highly Dynamic Energy Systems", Ph.D. Dissertation, Department of Mechanical Engineering, Virginia Polytechnic Institute and State University, Blacksburg, Virginia.
- Muñoz J. R., von Spakovsky M.R., 1999, "A Second Law Based Integrated Thermo-economic Modeling and Optimization Strategy for Aircraft / Aerospace Energy System Synthesis and Design (Phase I – Final Report)," final report, Air Force Office of Scientific Research, New Vista Program, December.
- Muñoz, J. R. and von Spakovsky, M. R., 2000, "The Use of Decomposition for the Large Scale Synthesis/Design Optimization of Highly Coupled, Highly Dynamic Energy Systems: Part I – Theory", *2000 ASME International Mechanical Engineering Congress and Exposition*, Orlando, Florida, November 5-10.
- Muñoz, J.R., von Spakovsky, M.R., 2001a, "A Decomposition Approach for the Large Scale Synthesis/Design Optimization of Highly Coupled, Highly Dynamic Energy Systems," *International Journal of Applied Thermodynamics*, March, vol. 4, no. 1.
- Muñoz, J. R. and von Spakovsky, M. R., 2001b, "The Application of Decomposition to the Large Scale Synthesis/Design Optimization of Aircraft Energy Systems", *International Journal of Applied Thermodynamics*, Vol. 4, No.2, pp. 61-76, June
- Muñoz, J.R., von Spakovsky, M.R., 2003, "Decomposition in Energy System Synthesis / Design Optimization for Stationary and Aerospace Applications," *AIAA Journal of Aircraft*, special issue, Vol. 39, No. 6, Jan-Feb.
- Olsson, B., von Spakovsky, M.R., Favrat, D., 1999, "An Approach for the Time-dependent Thermo-economic Modeling and Optimization of Energy System Synthesis, Design and Operation (Part I: Methodology and Results)," *International Journal of Applied Thermodynamics*, vol. 2, no. 3, pp 97-114.
- Oyarzabal, B., von Spakovsky, Ellis, M. W., 2003, "Optimal Synthesis/Design of a PEM Fuel Cell Cogeneration System for Multi-Unit Residential Applications – Part II: Application of a Decomposition Strategy," *Journal of Energy Resources Technology*, ASME transactions, N.Y., N.Y., submitted for publication.
- Rancruel, D. F. 2003 "A Decomposition Strategy Based on Thermo-economic Isolation Applied to the Optimal Synthesis/Design and Operation of an Advanced Fighter Aircraft System", Master thesis, Virginia Polytechnic Institute and State University, Blacksburg, VA.
- Rancruel, D. F., von Spakovsky, MR, 2003, "A Decomposition Strategy Applied to the Optimal Synthesis/Design and Operation of an Advanced Fighter Aircraft System: A Comparison with and Without Airframe Degrees of Freedom", Proceedings of the IMECE, Washington, D.C., November 16-21, 2003.
- Raymer D., 2000, Aircraft Design: A Conceptual Approach, AIAA educational series.
- von Spakovsky, M. R. and Evans, R. B., 1993, "Engineering Functional Analysis (Part I)", *Journal of Energy Resources Technology*, ASME Transactions, Vol. 115, No. 2, June.
- Zimering, B., Burnes, D., Rowe, J., 1999, "Gas Turbine Power Generation System Configuration Study and Optimization," 1999 International iSIGHT Users Conference, Chapel Hill, N.C., Oct 4-6.

